Domain wall displacement in Py square ring for single nanometric magnetic bead detection

P. Vavassori, V. Metlushko, B. Ilic, M. Gobbi, M. Donolato et al.

Citation: Appl. Phys. Lett. **93**, 203502 (2008); doi: 10.1063/1.3030984
View online: http://dx.doi.org/10.1063/1.3030984
View Table of Contents: http://apl.aip.org/resource/1/APPLAB/v93/i20
Published by the American Institute of Physics.

Domain wall displacement in Py square ring for single nanometric magnetic bead detection

P. Vavassori,[1,a)] V. Metlushko,[2] B. Ilic,[3] M. Gobbi,[4] M. Donolato,[4] M. Cantoni,[4] and R. Bertacco[4]
[1]*CIC nanoGUNE Consolider, 20018 Donostia-San Sebastian, Spain and CNR-INFM S3, CNISM and Dipartimento di Fisica, Università di Ferrara, 44100 Ferrara, Italy*
[2]*Department of Electrical and Computer Engineering, University of Illinois at Chicago, Chicago, Illinois 60607, USA*
[3]*Cornell Nanofabrication Facility, Cornell University, Ithaca, New York 14853, USA*
[4]*LNESS-Dipartimento di Fisica, Politecnico di Milano, Via Anzani 42, 22100 Como, Italy*

(Received 26 September 2008; accepted 31 October 2008; published online 17 November 2008)

An approach based on domain wall displacement in confined ferromagnetic nanostructures for attracting and sensing a single nanometric magnetic particle is presented. We modeled and experimentally demonstrated the viability of the approach using an anisotropic magnetoresistance device made by a micron-sized square ring of Permalloy. This detection concept can be suitable to biomolecular recognition and, in particular, to single molecule detection. © *2008 American Institute of Physics*. [DOI: 10.1063/1.3030984]

Intense research is presently directed toward the development of high sensitivity magnetoresistive sensors for the detection of magnetic beads because of their potential high impact on biochemical applications and diagnosis in medicine. Since the pioneering work by Baselt *et al.*[1] magnetic beads have been used for labeling and detecting target molecules at the surface of magnetic sensors where probe molecules are immobilized. High biological sensitivity can be achieved in immunoassays, theoretically down to the single molecule detection if nanobeads are employed. This is particularly appealing for biomedical research, offering the opportunity of immobilizing and detecting a biomolecule at a desired location for fundamental studies of its functions and dynamics.[2] A number of very sensitive magnetic field detection devices have been developed during recent years, which are able to detect a single micromagnetic particle, such as giant magnetoresistance (GMR) sensors,[1] spin-valves,[3] miniaturized silicon Hall sensors,[4] planar Hall effect sensors based on Permalloy thin films,[5] and tunneling magnetoresistance sensors.[6] The use of the anisotropic magnetoresistance (AMR) effect in ring-shaped sensors as sensitive bead detectors was suggested by Miller *et al.*[7] and more recently the approach has been extended by Llandro *et al.*[8] to ring-shaped multilayered (pseudo-spin-valve) sensors based on GMR. In some cases the possibility of detecting single nanometric beads has been foreseen.[9] However, to date, none of these approaches has experimentally demonstrated recognition of single nanometric magnetic beads with a diameter below 100 nm, particularly appealing for reducing the perturbation on the affinity between target and probe molecules.

Here we demonstrate the capability of detection of individual nanometric magnetic beads with a diameter of 80 nm previously attracted to the active sensing area of an AMR sensor based on a ferromagnetic micron-sized square ring. A salient feature of the sensor concept presented here[10] is that the entire device does not need to be as small as the nanobeads to be sensed, making its fabrication less challenging. In fact the nanometric size of the sensing area arises from the physical properties of a domain wall (DW) localized at a geometric corner. The concept illustrated in the present paper relies on a previous experimental work made on square rings of Permalloy (Py) for application in magnetic storage of information.[11] In this design head-to-head and tail-to-tail DWs having a transverse structure (Néel type)[11] can be positioned at a given corner, and their position can be read electrically thanks to the AMR effect: when a DW is present between two sensing leads a reduction in the resistance is observed since some of the magnetization of the DW points perpendicularly to the current flow. Otherwise, when there is no DW present between the two sensing leads, the magnetization follows the direction of the perimeter of the ring and the resistance is higher. In this work we adapted this device to demonstrate a detection concept suitable for the detection of magnetic nanobeads. Panel (a) of Fig. 1 shows the scanning electron microscopy image of the structure used in the present experiment. The 30 nm thick Py square ring structures have been lithographically patterned on top of 20 nm thick and 100 nm wide Au contacts, previously fabricated on a SiO_2/Si substrate. The outside size of the rings is $1.0 \times 1.0\ \mu m^2$, the width of each segment is about 180 nm, and the slit is about 80 nm wide. For the magnetoresistance measurements presented here, the voltage drop was measured using a lock-in amplifier between contacts labeled 3 and 4 in the panel (a) of Fig. 1, with a current of 15 μA injected at contact 1 while contact 2 was grounded. The three-dimensional (3D) schematic shown in panel (b) of Fig. 1 illustrates the sensing concept proposed here: when a bead is placed over a DW previously positioned at one corner of the ring structure and a magnetic field H is applied to displace the DW along one ring edge, a magnetic dipole moment $\boldsymbol{\mu}$ is generated in the superparamagnetic bead, as shown in Fig. 1. The stray field generated by $\boldsymbol{\mu}$ opposes the applied field below the bead, causing an increase in the value of the field **H** required to displace the DW. In panel (c) of Fig. 1 we present the result of a simulation of the effect when a magnetic nanobead (a commercial MICROMOD nanomag®-D with diameter 130 nm and magnetic moment $\mu \approx 150 \times 10^{-15}$ emu at 1000 Oe) is placed over the DW at a vertical distance of 15 nm from the surface of the Py structure. 3D micromagnetic

a)Electronic mail: p.vavassori@nanogune.eu.

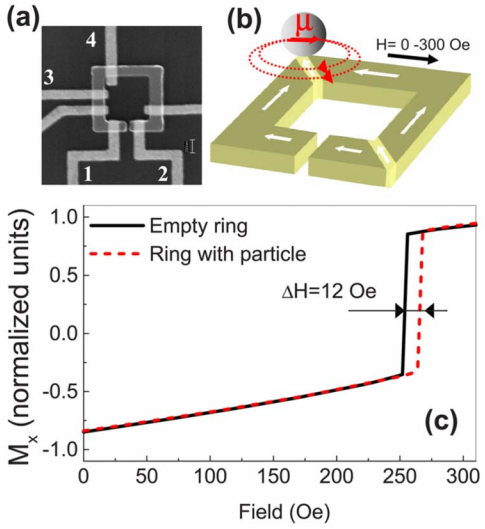

FIG. 1. (Color online) Panel (a): SEM image (2.5×2.5 μm^2) of the device structure. Panel (b): 3D schematic of the ring with two DWs in the top-left and bottom-right corners and with a magnetized nanoparticle of moment μ producing a stray field in the top-left corner. Panel (c): DW displacement field calculated without (solid line) and with (dashed line) a magnetic particle of 130 nm placed at a distance of 15 nm over the corner with a DW. The magnetic field is applied as shown in panel (b). In the calculations we used a computational cell of $10\times10\times15$ nm^3 and the standard material parameters for Py.

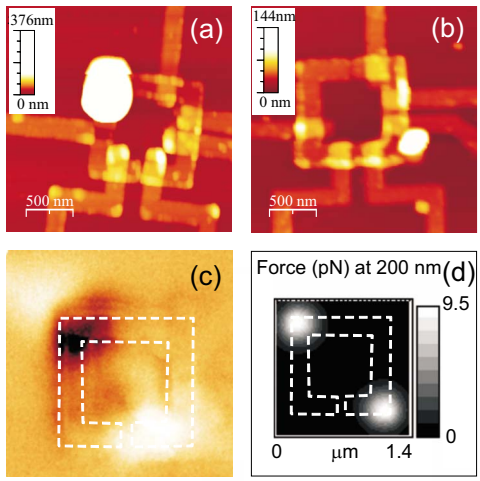

FIG. 2. (Color online) AFM images from rings capped with 30 nm of SiO_2 after beads have been dispensed in solution on the chip surface: (a) cluster of 50 nm beads and (b) single 130 nm bead. The diagonal lines indicate the position of the DW. Panel (c): MFM image from a ring after initialization with DWs at the top-left and bottom-right corners. Panel (d): simulation of the focusing magnetic forces on a plane at 200 nm distance from the ring surface. The dashed lines in panels (c) and (d) are guide for the eyes.

simulations of the whole system were performed by using the object oriented micromagnetic framework (OOMMF).[12] In detail, the graphs in Fig. 1(c) show the variation in the magnetization component parallel to the applied field, normalized to its saturation value in the upper segment of the ring as a function of the external field used to displace the DW, without (solid line) and with (dashed line) a bead over the structure. The simulations show that due to the proximity of the bead, the displacement of the DW is retarded by 12 Oe with respect to the case of the ring alone [compare dashed with solid line in Fig. 1(c)], hereby demonstrating the potential for the utilization of this sensing concept for the detection of individual nanometric magnetic beads.

A condition to be fulfilled for the correct operation of the device is that the nanoparticle is placed exactly over one corner of the ring structure. This is a problem common to all the magnetoresistive sensors oriented to single molecule detection developed so far for which an external action (magnetic fields and micromanipulators) is required to place and magnetize the particle for an optimal detection. Our approach has the advantage that no external action is needed to place the bead over the corner, viz., the active area of the sensor, thanks to magnetic self-focusing on the DW. This is illustrated in panels (a) and (b) of Fig. 2, which show atomic force microscopy (AFM) images taken from the ring structure after having first placed a transverse DW in two opposite corners of the ring and subsequently dispensed the beads on the chip surface. The latter was capped with a 30 nm thick SiO_2 layer to avoid any local specific chemical interaction between beads and the different materials of the sensors. We typically dispensed a 1 μl drop in solution of beads in ethanol with a final concentration of about 10^6 particles/μl and then immediately dried the surface with nitrogen. We employed two types of commercial nanobeads, MACS™ and nanomag®-D, having diameters of 50 and 130 nm. The AFM image in panel (a) refers to the 50 nm beads and shows that a cluster of several beads is formed over one of the corner where a DW is located. The AFM image in panel (b) shows a single 130 nm bead placed over the opposite corner, where the other DW is located. We repeated the experiment several times changing either ring structure or the DW position and we always observed that clusters (most common for the 50 nm beads) or single particles are found over the corners where the DWs are located, but never over the other two corners of the ring. This interesting behavior can be understood by looking at the magnetic force microscopy (MFM) image in panel (c) of Fig. 2, showing that there is a magnetic field emanating from the structure only in correspondence of the DWs (left-top and bottom-right corners in the image). Elsewhere the field is negligible. The strong field gradient that characterizes this stray field causes a self-focusing action that can trap and drag toward the corner sensing region a nanoparticle flowing in the vicinity of the structure. The force acting on a nanoparticle at a certain distance from the ring surface can been calculated by computing with OOMMF the magnetic field **H** created in the surrounding space by the nanostructure in the magnetic configuration with a DW at the two opposite corners of the ring. Then the following vector expression is used for the force: $\mathbf{F}=-\mu_0(\boldsymbol{\mu}\cdot\nabla)\mathbf{H}$, where $\boldsymbol{\mu}=\mu(\mathbf{H})\mathbf{h}$ with $\mu(\mathbf{H})$ the known magnetization curve of the bead and **h** is a unit vector parallel to the field **H**. Panel (d) of Fig. 2 shows the contour plot of the modulus of the attractive force acting on a nanobead of 130 nm in diameter computed in a plane at 200 nm from the sensor surface. The plot shows that a force in the range of 0.1–10 pN is acting on the bead over an area of about 400 nm in diameter, assuring an effective trapping and focusing action on the nanobead.

Figure 3 shows the results of the magnetoresistance measurements carried out to verify the sensing concept presented here onto rings without SiO_2 capping. Panel (a) shows the AFM image taken from a clean ring, while panel (b) shows the AFM image of the same ring after the dispensation of beads of 130 nm diameter (MICROMOD nanomag®-D) in ethanol and rinsing with de-ionized water for 1 min. In panel (b) the white line indicates the position of the DW in the

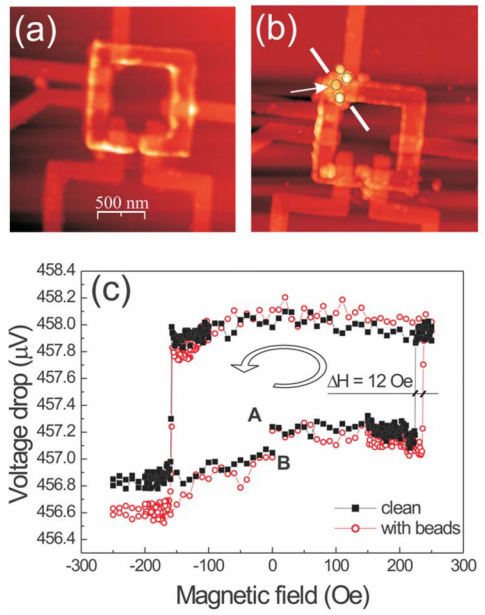

FIG. 3. (Color online) AFM images from a (a) ring clean and (b) after beads dispensation. In panel (b) the white line indicates the position of the DW, while circles put in evidence four beads positioned in the proximity of the corner; the arrow indicates the bead substantially affecting the DW displacement field according to micromagnetic simulations. Panel (c): voltage drop across the corner as a function of the magnetic field for the same ring clean (squares) and with beads on top (circles). Labels A and B mark the beginning and the end of the acquisition, respectively.

top-left corner of the ring structure, while the circles evidence that the original particles have broken up into four smaller beads, having an average diameter of about 80 nm, placed over and next to the corner. Fragmentation revealed to be relevant for the present experiment because a strong chemical interaction between the beads and the sensor surface took place, keeping the beads at a fixed position during measurements. Panel (c) of Fig. 3 shows the voltage drop measured across the corner [leads 2 and 3 in Fig. 1(a)] where the DW is initially positioned, as a function of the magnetic field **H** applied parallel to the upper edge of the ring for the ring without (square symbols) and with (circles) beads on top. The first transition observed in the voltage signal (resistance increase) when **H** is increased from 0 to 250 Oe corresponds to the displacement of the DW from the top-left to the top-right corner of the ring, while the second transition (resistance decrease), occurring when **H** is subsequently reduced to −250 Oe, corresponds to the DW being brought back to the initial position. The magnetoresistance measurements show that due to the proximity of the beads, the displacement of the DW from the top-left to the top-right corner is retarded by 12 Oe [$\Delta\mathbf{H}$ in Fig. 3(c)]. The fact that no variation in the DW displacement field is observed when the DW is brought back to the initial corner (transition for negative fields in Fig. 3) confirms that $\Delta\mathbf{H}$ is due to the presence of the beads next to the initial corner and not to instrumental artifacts as, e.g., a nonperfect control of the applied magnetic field. Magnetoresistance measurements after removal of the four beads gave exactly the same result obtained on the ring before dispensation (curve with squares of Fig. 3), thus demonstrating the reliability of the observed change in the displacement field and the viability of the sensing concept proposed here. Micromagnetic simulations of this geometry with four fragments of beads placed as in the experiment give a shift in the displacement field of the order of 12 Oe in agreement with the experimental value. This is obtained for the minimum beads-sensor distance compatible with the mesh (15 nm), while this value is unaltered when increasing the distance up to 30 nm. Simulations also indicate that only the two beads over the DW have an influence, with the bead exactly on top of the DW (indicated by the arrow in Fig. 3) that is essentially responsible of the shift of 12 Oe, while the other one gives a contribution of only 2 Oe. In this sense our experiment demonstrates the detection of two beads, and also the possibility of single bead detection as the error in the evaluation of the displacement field is ± 2 Oe. Moreover simulations show that the reduction in the width of the ring to the nanobead diameter doubles the value of $\Delta\mathbf{H}$. This in conjunction with the use of nanobeads of a higher magnetic moment (values up to 5 times that of the beads used here are reported in the literature) can increase the achievable value of $\Delta\mathbf{H}$ by about ten times.

To summarize we demonstrated the viability of an approach for sensing single nanometric beads based on their impact on the displacement field of a DW at a corner of a Py nanostructure. The self-focusing effect on the active sensor area due to the strong magnetic field emanating from the DW has also been demonstrated. This proof of concept paves the way to the optimization of the sensor geometry for improving sensitivity and fulfilling the requirements imposed by biological recognition in view of application to single biomolecule detection and localization.

The authors thank P. Fraternali, M. F. Hansen, S. Brivio, and D. Petti for fruitful discussion and M. Leone for his skillful technical support. V.M. acknowledges support by the U.S. NSF, Grant No. ECCS-0823813, and by the U.S. Department of Energy, Office of Science, Office of Basic Energy Sciences, under Contract No. DE-AC02-06CH11357 (CNM ANL Grant Nos.468 and 470). P.V. acknowledges funding from the Department of Industry, Trade, and Tourism of the Basque Government, the Provincial Council Gipuzkoa under the ETORTEK Program (Project No. IE06-172), the Spanish MICINN (Project No. CSD2006-53), and the EU VII Framework Programme (Grant Agreement No. PIEF-GA-2008-220166).

[1]D. R. Baselt, G. U. Lee, M. Natesan, S. W. Metzger, P. E. Sheehan, and R. J. Colton, Biosens. Bioelectron. **13**, 731 (1998).
[2]A. Ishijima and T. Yanagida, Trends Biochem. Sci. **26**, 438 (2001).
[3]G. Li, V. Joshi, R. L. White, S. X. Wang, J. T. Kemp, C. Webb, R. W. Davis, and S. Sun, J. Appl. Phys. **93**, 7557 (2003); D. L. Graham, H. Ferreira, J. Bernardo, P. P. Freitas, and J. M. S. Cabral, *ibid.* **91**, 7786 (2002).
[4]P. A. Besse, G. Boero, M. Demierre, V. Pott, and R. Popovic, Appl. Phys. Lett. **80**, 4199 (2002).
[5]L. Ejsing, M. F. Hansen, A. K. Menon, H. A. Ferreira, D. L. Graham, and P. P. Freitas, Appl. Phys. Lett. **84**, 4729 (2004).
[6]W. Shen, X. Liu, D. Mazumdar, and G. Xiao, Appl. Phys. Lett. **86**, 253901 (2005).
[7]M. M. Miller, G. A. Prinz, S.-F. Cheng, and S. Bounnak, Appl. Phys. Lett. **81**, 2211 (2002).
[8]J. Llandro, T. J. Hayward, D. Morecroft, J. A. C. Bland, F. J. Castaño, I. A. Colin, and C. A. Ross, Appl. Phys. Lett. **91**, 203904 (2007).
[9]G. Mihajlović, P. Xiong, S. von Molnár, M. Field, and G. J. Sullivan, J. Appl. Phys. **102**, 034506 (2007).
[10]R. Bertacco and P. Vavassori, Italian Patent Application No. TO2008A000314 (23, April 2008).
[11]P. Vavassori, V. Metlushko, and B. Ilic, Appl. Phys. Lett. **91**, 093114 (2007).
[12]M. J. Donahue and D. G. Porter, *OOMMF User's Guide, Version 1.2 Alpha 3* (NIST, Gaithersburg, MD, 2002).